Talanta 217 (2020) 120994

Contents lists available at ScienceDirect

Talanta

journal homepage: www.elsevier.com/locate/talanta

Detection of quiescent fungi in harvested fruit using CMOS biosensor: A proof of concept study

Dolev Zamir, Ortal Galsurker, Noam Alkan, Evgeni Eltzov*

Department of Postharvest Science of Fresh Fruit, Volcani Center, Agricultural Research Organization, Rishon LeZion, 7505101, Israel

ARTICLE INFO

Keywords:
mRNA
Quiescent
CMOS-Biosensor
Fungus
Colletotrichum
Food-loss

ABSTRACT

Postharvest fruit decay is caused by fungal pathogens and leads to major losses. In this study, specific mRNA sequences that are upregulated in the fungus *Colletotrichum gloeosporioides* during its quiescent stage in fruits, were identified using a CMOS sensor. The identification process was based on sandwich approach, where strands complementary to the *C. gloeosporioides* mRNA sequences (quiescent stage-specific) were immobilized on the CMOS surface, and exposed to the target complementary reporter strands. In the presence of a target sequence, the reporter strand (linked to the enzyme horseradish peroxidase (HRP)) was left in the system and a measurable light signal was produced. The complementary strands specifically anneal to the mRNA in the sample. The sensitivity of the technology was assessed by mRNA sequences isolated from *C. gloeosporioides*, and identified as 10 nM RNA. The effect of the pathogenicity state on the sensor performance was also evaluated. The CMOS sensor could detect quiescent fungi, which are barely detectable by other means. The unique capability of the proposed system to detect and recognize the fungus during both pathogenic and quiescent stages, will allow the development of new sensors that can monitor the amount of undetectable quiescent fungi in harvested fruit, enabling improved food management.

1. Introduction

Postharvest food loss is a major issue. It is estimated at 40%–50% of harvested crops worldwide, mostly due to physiological deterioration and rots caused by fungi [1]. In addition to spoilage processes, toxic compounds produced by pathogenic microorganisms may pass to food and cause significant health damage to humans and animals [2]. For future food safety and to mitigate food losses, presence of the fungus should be monitored after harvest and during the supply chain. Generally, the conventional technologies for detecting postharvest pathogenic fungi (PCR and ELISA [3]) are sensitive and precise, but are costly and includes complicated protocols, which makes these applications less optimal for agricultural use. Furthermore, while they can indicate the presence of these microorganisms in the crops, there is no evaluation of their pathogenicity state. Fungi from several genera may cause postharvest decay of fresh produce [4–6]. Usually, after penetrating the immature fruit, the fungi remain quiescent, and only switch to pathogenic state after storage and ripening, initiating the active attack. The quiescent infections are microscopic and cannot be visually detected during packaging or subsequent transport [7–9]. Thus, there is a huge demand for sensitive, inexpensive and simple applications, which will not only detect the presence of the microorganisms in the crops after decay, but also evaluate their presence during their quiescent stage.

With over 470 widely distributed host genera (mango, avocado, and strawberry, to name a few), *Colletotrichum gloeosporioides* is one of the most common disease agents in harvested fruit [10]. After conidial germination, *C. gloeosporioides* usually passes through three lifestyle stages: appressoria (penetration), quiescence (latent stage), and the necrotrophic stage, which causes decay. In the first stage, C. *gloeosporioides* penetrates into the fruit cuticle, and it remains there in an extended quiescent state until the fruit ripens [9]. At fruit ripening, the fungal pathogen switches to the necrotrophic stage, resulting in anthracnose disease in the fruit [10]. During these different stages, the fungal pathogen significantly upregulates stage-specific transcripts [10]. These mRNA transcript sequences can be used as markers for fungal pathogenicity stage.

A biosensor for RNA detection may be the easiest, cheapest and fastest method to recognize the presence of pathogens in crops. Typically, biosensors are built from three parts—bioreporter, transducer, and interface, the latter immobilizing the first part on the second. Mass balance [11,12], optical and quartz crystal microbalance [13,14] are amongst the most common measurement approaches for DNA detection. Recent advances in the optical field have led to the development of sensitive, low-cost and small-size photodetectors,

* Corresponding author.
E-mail address: eltzov@volcani.agri.gov.il (E. Eltzov).

https://doi.org/10.1016/j.talanta.2020.120994
Received 16 February 2020; Received in revised form 29 March 2020; Accepted 31 March 2020
Available online 07 April 2020
0039-9140/

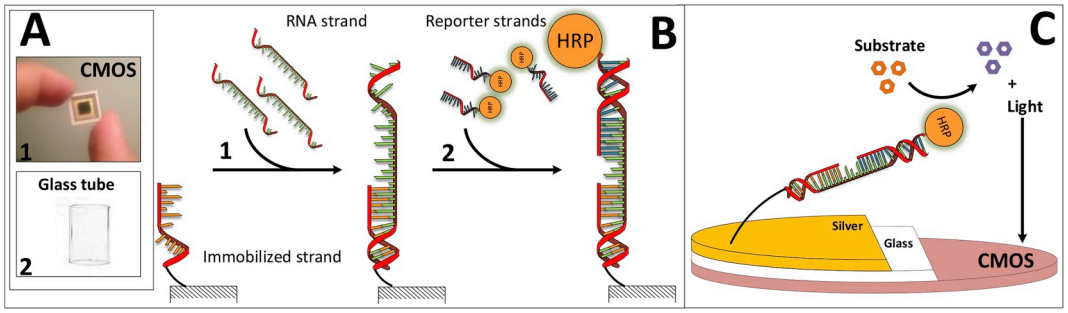

Fig. 1. Schematic representation of the CMOS-based biosensor and the measurement procedure. The proposed system is based on a CMOS photodetector (A1) and a glass tube (A2) with silver nanoparticles modified with immobilized DNA. A complementary RNA sequence in the sample will anneal specifically to the surface-immobilized RNA on the one side (B1) and to the complementary reporter strand linked to horseradish peroxidase enzyme on the other side (B2). After substrate addition, the horseradish peroxidase enzyme linked to the reporter strand will produce light. This light will be detected by the CMOS sensor (C) and represented as measurable light values.

which are based on complementary metal-oxide-semiconductor (CMOS) technology [15]. Such CMOS technology have shown unique properties for the construction of portable platforms. CMOS-based biosensors have been used for bacterial detection [16,17], in environmental air and water samples for toxicity evaluation tests [18,19], and as PCR-process monitoring tools [20,21]. More importantly, CMOS-based applications were found to be valuable for food safety evaluation [22–26]. Compared to the environmental and food-safety fields, only few CMOS based biosensors have been proposed for agriculture use [27,28]. In this study, specific mRNA sequences that are upregulated in *C. gloeosporioides* during its quiescent stage [10] were incorporated into a CMOS biosensor. The identification process was based on sandwich approach, where strands complementary to the *C. gloeosporioides* mRNA sequences were immobilized on the CMOS surface. In the presence of the target analyte, these complementary strands specifically anneal to the mRNA in the sample. The quantity of *C. gloeosporioides* quiescent mRNA sequences was then evaluated with a reporter strand that anneals to another position on the quiescent mRNA (Fig. 1). This creates a surface complex that includes mRNA and reporter strands, which remains on the CMOS surface after the washing steps. Signal generation is then assessed by a luminescent enzymatic reaction of horseradish peroxidase (HRP) enzyme that is conjugated to the reporter strand. This technology not only allows pathogen detection in fresh agricultural produce, it also identifies the unseen quiescent fungi inside the fruit [29].

2. Materials and methods

2.1. Chemicals

Hydrochloric acid (HCl) 37% (#953503) and Hydrogen peroxide (H_2O_2) (#2186–1) were purchased from J.T. Baker (Phillipsburg, NY, USA). Methyl alcohol (#6712) was purchased from Macron (Center Valley, PA, USA). 3-Glycidoxypropyltrimethoxysilane (#440167) and Tris-EDTA (#101903432) were purchased from Sigma-Aldrich (Rehovot, Israel). Silver nitrate coating: D-Glucose (#FG/0500/60), silver nitrate (#7761-88-8) and sodium hydroxide (#FS/4880/60) were purchased from Fisher Chemical (Fair Lawn, NJ, USA). Ammonium hydroxide (#033285.1) was purchased from Alfa Aesar (Lancashire, UK). The DNA sequences were purchased as described in Table 1.

2.2. Surface activation

To activate the sensor surface, 350-µL flat-bottom glass tubes (CSI, #I025-630) were incubated in MeOH:HCl solution (1:1, v/v) at room temperature for 20 min. Then the tubes were dipped in double-deionized water (DDW) and later sonicated in a sonication bath (JK-OCD30A, MRC, Holon, Israel) for 20 min. The tubes were exposed to piranha solution (H2O2:H2SO4, 3:7, v/v) at 90 °C for 60 min. Then they were rinsed with DDW, dried with N_2 and exposed to 3-glycidoxypropyltrimethoxysilane at 60 °C for 60 min. Finally, the tubes were rinsed with DDW, dried and subjected to silver-deposition procedures.

2.3. Silver deposition

Silver liquid deposition was performed as previously described [30]. Briefly, 500 µL fresh 5% (w/v) NaOH solution was added to a silver nitrate solution (0.22 g in 26 mL of DDW) with rapid stirring. After the formation of a dark-brownish precipitate, up to 1 mL of ammonium hydroxide was added to the deposition solution, until the precipitate dissolved. The clear solution was cooled to 5 °C by placing the it in an ice bath. Tubes were placed in the silver deposition solution, and fresh D-glucose solution (0.35 g in 4 mL of water) was added, then the mixture was stirred for 2 min. Later, the solution was heated to 30 °C. The tubes were incubated in the deposition solution until a silver layer was formed on the glass surface, then rinsed with water and dried.

2.4. Fungal inoculation and sample preparation

Single-spore cultures of *C. gloeosporioides* (isolate Cg-14) obtained from decayed avocado fruit were cultured on M_3S. The cultures were incubated at 24 °C in a shaking incubator at 150 rpm for 3 days. They were later harvested by filtration through a sterile Büchner funnel fitted with Whatman filter paper and rinsed with water. The hyphal mat was collected under liquid nitrogen and stored at −80 °C. Freshly harvested mature green and red tomato fruit (*Solanum lycopersicum* L.) were used for inoculation as previously described [10], with minor modifications. The mature green tomato was inoculated with 7 µL of a conidial suspension (5×10^5 conidia mL^{-1}), at 50 inoculation spots per fruit, with six different fruit per biological replicate and 10 biological replicates per treatment. RNA for the appressorium and quiescent stages was collected 19- and 100- hours post-inoculation of the mature green tomato fruit, respectively. For necrotrophic-stage growth, red fruit was punched with a needle to 1-mm depth and inoculated with 7 µL of a conidial suspension (5×10^5 conidia mL^{-1}). Six inoculation spots on each of six different fruit were inoculated per biological replicate, with 10 biological replicates per treatment. RNA for necrotrophic-stage evaluation was collected 48 h post-inoculation by removing tissue to 0.5 mm depth. All of the collected tissues were stored at −80 °C.

2.5. RNA extraction

RNA was extracted from 50 mg (fresh weight) of Cg-14 mycelium that was grown for 10 days on M_3S plates, or 100 mg of inoculated tomato fruit tissue from the three different stages (appressorium, quiescent, necrotroph). All of the samples were ground in liquid

Table 1
DNA sequencing.

Description	Sequence	Company
Reporter strand reverse complementarity sequence to the quiescent marker (Cgl_00014,454, enoyl-CoA-hydratase/isomerase)	HRP – 5′-TGA GGC GTG GGA AGC AAC-3′	Eurogentec (Seraing, Belgium)
Surface-strand	5′-TGG CTC GCC TTA GAC AGT CC-3′-SH	HyLabs (Rehovot, Israel)
Thiolated DNA sequences with conjugated fluorescein isothiocyanate	FITC – 5′-ATG CAC CGT AGC GAC CAG AG-3′-SH	
Positive target of the quiescent marker	5′-CCC AAG CTC ATA GGA CTG TCT AAG GCG AGC CAC GTC ACG ACC ACT GGA GAC GTG TAT CCC GTC ACC GAT CCA CTC GTC AAT GGG CTG TTC TCA AAG TTG CTT CCC ACG CCT CAA CAC ACA GTC-3′	
Negative target sequences of Cgl_00010,698 (pectate lyase) and Cgl_00010,395 (secretory lipase), respectively	5′-TCG TCT TGG GTC TCT GGT CGC TAC GGT GCA TCT CTC ATG CGC TCA GTC TCT GTG AGA CGC GAG TGA ACT TCG TTT TAC TGG TTA AAG AAC GGG GAA GGA AGA CAA CGA ACC ACG ACT ATT TCT-3′ and 5′-TGG AAG TCC GGT CCA TGC TCG CGT GTA TCC TGA TAT GGG ACA CGG CCA GGT TTT GGA GGC CGC CAG GGC TGA TAT CGC TGC TTG GAT CGC CGC GAG ATT TGA AGG AGT TCC CGT TGA GAA GAC-3’	

nitrogen to a fine powder using a mortar and pestle. RNA was extracted from Cg-14 mycelium using the Norgen Biotek Plant/Fungi Total RNA Purification Kit (Thorold, Canada) according to the manufacturer's protocols with 50 mg of the ground mycelium per isolate as the starting material. For the RNA extraction from inoculated tomato fruit, total RNA was isolated from 100 mg inoculated tomato fruit at each of the three stages, using the Spectrum™ Plant Total RNA Kit (Sigma Aldrich, STRN250-1 KT), by following the manufacturer's protocol. The purity of the extracted RNA was assayed with an ND-1000 spectrophotometer (NanoDrop Technologies, Thermo Scientific, Wilmington, DE, USA), and the extracts were stored at −80 °C before further analysis.

2.6. DNA immobilization

The DNA was immobilized on the glass surface by exposing the silver-modified tubes to 20 μL of 1 μM surface-DNA solution diluted with Tris-EDTA buffer for 1 h at room temperature in the dark. Then, the tubes were rinsed with Tris-EDTA buffer and exposed to 20 μL of target and reporter strands. Conventional PCR was performed using a Veriti 96-Well Thermal Cycler (Applied Biosystems) with one thermal program cycle (60 s at 90 °C, then 30 s at 75 °C, 30 s at 65 °C and finally 30 s at 53 °C). DNA quality and quantity were measured in the ND-1000 spectrophotometer. After exposure, the tubes were rinsed with Tris-EDTA buffer and placed on the CMOS sensor or in an in-vivo imaging system (IVIS-100, PerkinElmer, Waltham, MA, USA) for further light monitoring.

2.7. Instrument setup and signal measurement

The enzymatic activity was monitored using a specifically designed field-operable biosensor. The CMOS sensor [ULS solution kit by Anitoa (Palo Alto, CA)] was placed in a light-tight box to prevent possible light interference. The data was collected and analyzed using a specific software that was developed by Anitoa, which enabled the monitoring of the luminescent signal and the handling of the data in real-time measurement. A special holder preventing tube movement during the measurement procedure was combined inside the sensor setup. The light activation from the enzymatic reaction was observed by the deposition of 20 μL substrate solution (Luminol:H_2O_2, 1:1, v/v) on the CMOS sensor surface, and later placing the sample tubes above it.

2.8. Effect of tube surface location and dithiothreitol (DTT)

The effect of the tube surface location on the silver-deposition efficiency was examined. Both inner and external tube surfaces were activated as described in section 2.3. Then, the tubes were exposed to the silver deposition solution for different time periods (0, 7, 8, 10, 13 and 15 min) as described in section 2.3. Later, the tubes were rinsed, dried and photographed with a cellphone camera (Samsung, SM-G955F, Korea). The effect of DTT on DNA deposition on the silver surface was also examined. The immobilization efficiency was tested by adding 2.5 mM DTT to the DNA-immobilization solution (thiolated DNA sequences with conjugated FITC). DNA solutions, with and without DTT, were incubated with the tubes for 1 h at room temperature. Then, the tubes were rinsed with Tris-EDTA and analyzed by IVIS-100.

2.9. Sensitivity and specificity tests

The sensitivity of the CMOS-based sensor was determined by using tubes with immobilized DNA, which were incubated with different target DNA concentrations (100, 10, 1, 0.5, 0.3, 0.25 and 0.2 nM), as described in section 2.6. Then, the tubes were rinsed, dried and measured by using the CMOS sensor as described in section 2.7. The specificity of the CMOS-based sensor was determined as described in section 2.5, with the exposure step consisting of one positive and two negative target sequences. The tubes were rinsed, dried and measured by using the CMOS sensor as described in section 2.7.

2.10. Detection of fungus at different pathogenic stages

The effect of the fungal pathogenicity state on the sensor response was determined by exposing the tubes to different mRNA extractions (section 2.5). As previously described in section 2.6, 20 μL extract was mixed with 20 μL reporter solution (100 nM), and then incubated at different temperatures. Later, the tubes were rinsed and measured by using the CMOS sensor (section 2.7).

2.11. Reproducibility of the system and statistical analysis

For each experimental stage, a minimum of 30 separate and different setups were exposed to the examined parameters. Two-way repeated-measures analysis of variance (ANOVA) was employed, in order to evaluate the differences between the tested parameters (i.e., different DNA sequences in the system-specificity experiments, different target DNA concentrations in the sensitivity experiments and differences in the pathogenicity stages (appressorium, quiescence, necrotrophic).

3. Results and discussion

3.1. Optimization of the immobilization process

One of the main challenges in DNA-based sensor development is the immobilization of the receptor molecules onto the solid-phase transducer. The bioreporter molecules at the top of the sensor not only need to retain their activity after the immobilization step, but they also have to remain sensitive and specific to the target analyte. In this study, the DNA strands that were immobilized onto the glass surface had to bind

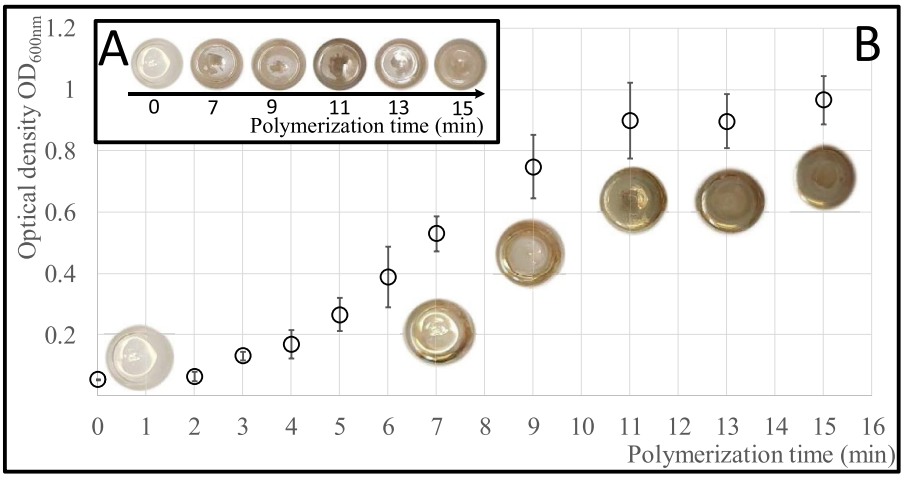

Fig. 2. Effect of the silver-deposition reaction over time on silver immobilization on the internal (A) and external (B) surfaces of the tube.

the complementary target RNA strands within the sample, and then complete the hybridization process with the reporter strand on their opposite end (Fig. 1). The first step of the immobilization process was to bind the DNA strands onto the silver-modified glass surface. Two different deposition locations in the tube were chosen (i.e., inside and outside the tube surface). First, the effect of the reaction time on the deposition efficiency was tested (Fig. 2). The silver-modification process is a kinetic reaction in which the layer formation depends on the exposure time of the glass surface to the deposition solution [31,32]. However, no visible correlations were observed between deposition time and silver uniformity on the inner surface (Fig. 2A). This might have been due to the difficulty in controlling all of the surface activation and modification conditions (i.e., rinsing and drying steps, exposure temperatures and times) during the glass-activation and silver-deposition processes in the small inner tube volume. Moreover, the tube structure also makes it difficult to proceed with the rinsing and drying steps, which are critical for effective treatment. Therefore, residual water and chemicals may interfere with further silver deposition. Another possible reason for the non-uniform deposition is the inability to control the reaction temperatures inside the tube. Therefore, external surface modifications were also examined. The external tube surface, in this case, is more convenient for an efficient rinsing and drying, and the solution temperature can be easily controlled for optimal modification procedures. Indeed, in this case, similarly to previous studies [33], increasing exposure time induced silver deposition and created more uniform layers (Fig. 2B). Thus, the external surface-modification procedure was chosen for further experiments.

Additional parameters were evaluated in order to optimize the deposition protocol, such as the effects of deposition temperature, stirring intensity during the immobilization process, and chemical concentration (data not shown). In addition, the effect of DTT, a small-molecule redox reagent used as a reducing or “de-protecting” agent for thiolated DNA [34], on the surface-immobilization efficiency was tested. DTT is usually added to thiolated DNA in order to lower or prevent coupling self-reactions between the terminal sulfur atoms, and it is used in chemistry, biochemistry, peptide–protein reactions and clinical medicine applications [35]. In this study, adding DTT to the DNA incubation solution not only changed the morphology of the silver (e.g., color and opacity) (Fig. 3D) but also had a negative effect on the DNA-immobilization efficiency (Fig. 3E). In contrast to the glass surface treated only with DNA (Fig. 3C), there were no visible responses from tubes exposed to the DNA–DTT solution (Fig. 3E). This might be due to an interaction between the silver surfaces and DTT, which is a strong reducing agent, with a redox potential of −0.33 V at pH 7 [36]. It is known that DTT, as well as other SH-containing compounds, strongly bind to silver atoms [37]. Thus, the observed inhibitory effect might be explained by DTT binding to the silver nanoparticles, thereby preventing further DNA immobilization. Changes in the silver color of the samples with DTT supported this assumption (Fig. 3D). Thus, all further immobilization procedures were performed without adding DTT to the incubation solution.

3.2. Specificity of the CMOS system to the target strands

Specificity of the CMOS-based system was assessed using mRNA sequences isolated from *C. gloeosporioides* (as described in sections 2.4 and 2.5) that were upregulated during the quiescent stage [9]. For each experiment, the biosensor was operated with three different strands, i.e., surface, target, and reporter with conjugated HRP. This measuring technology is based on specific nucleic acid hybridization of the immobilized DNA probe on the sensor. Analyte DNA and reporter strands have been widely used to detect bacteria, fungi and genetically modified organisms [38,39]. The rationale is that the signal will only be generated in the presence of the target analyte in the sample, which will anneal to the surface DNA strand from one side and to the reporter strands in its opposite direction. The sensor's ability to distinguish between *C. gloeosporioides* mRNA that is upregulated during the quiescent stage and other tested strands was confirmed by specificity trials (Fig. 4). The specificity of the proposed device was demonstrated by differences between the responses of the sensor to the complementary strand (Fig. 4B) and the noncomplementary DNA strands (Fig. 4A and C, Cgl_00010,698 and Cgl_00010,395, respectively). A much higher signal was observed in response to the complementary DNA sequence of the quiescent stage-upregulated transcript (Cgl_00014,454), enabling a precise distinction between the specific and nonspecific sensor responses (Fig. 4).

3.3. Sensitivity and efficiency of the CMOS system

The sensitivity of the proposed system was evaluated by exposing the modified tubes to the mixtures with a constant concentration (100 nM) of the quiescent-stage reporter and a constant concentration (100 nM) of surface strands and different concentrations of the target RNA strand. The results presented in Fig. 5 demonstrate the ability of the sensor to distinguish between different concentrations of the target RNA strand molecules in solution above a 5 nM threshold of the target sequence. The proposed CMOS application provided similar sensitivity to many other optical-based [40,41], electrochemical-based [42,43] and mass-balance-based [44,45] biosensors for pathogen detection in plants, while the PCR technology enables a more sensitive DNA

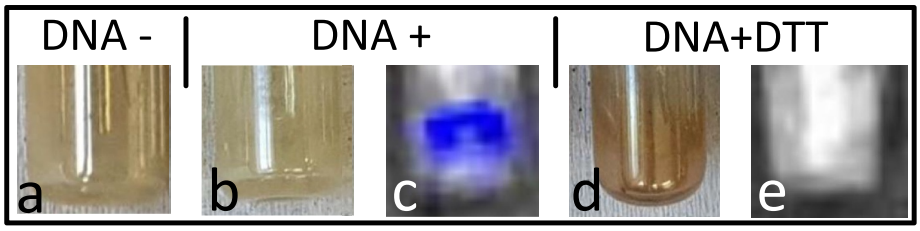

Fig. 3. Effect of dithiothreitol (DTT) on tube-surface stability and DNA immobilization efficiency. Tubes were modified with a silver layer (A) and incubated with thiolated DNA without (B and C) and with (D and E) DTT. While (A), (B) and (D) show changes in the surface morphology, (C) and (E) show DNA fluorescence as a factor of immobilization efficiency.

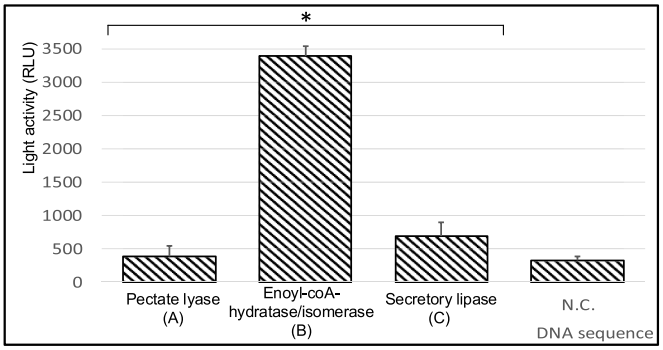

Fig. 4. Specificity of the system to (A) a nonspecific DNA sequence (Cgl_00010,698; pectate lyase), (B) a specific DNA sequence (Cgl_00014,454; enoyl-CoA-hydratase/isomerase) and (C) a nonspecific DNA sequence (secretory lipase; Cgl_00010,395). A negative control (N·C.) shows the response of the device to a synthetic DNA. *P < 0.005 by ANOVA. RLU, relative light units.

detection. An additional advantage of the CMOS-based application is the active-pixel sensor technology, where each picture element (pixel) has a photodetector and an active amplifier [46]. This not only increases the sensitivity of the sensor, but also provides better visualization of the light activity on the surface of the tubes during the measurement process. This effect can be seen in Fig. 5B, with brighter zones above the tube surface and their quantification in Fig. 5A. Furthermore, at all higher tested concentrations (up to 10 nM), the tube dimensions were easily visualized by similar light activities above the tube surface.

3.4. Application of the CMOS system to in-vivo evaluation

The CMOS-based sensor development for the detection of quiescent-stage fungi in fruit required also the evaluation of the RNA of the peel at different *C. gloeosporioides*-infection stages. The CMOS biosensor was exposed to RNA extracted from tomato fruit inoculated with *C. gloeosporioides* at different developmental stages. Postharvest fungal pathogens usually penetrate the fruit before harvest. The fungi then enter into a long quiescent and microscopic phase in the immature fruit; when the fruit ripens, the fungi then switch to their necrotrophic stage and cause decay [9,10]. For this CMOS biosensor proof of concept, the focus was on detecting the fungus during its microscopic quiescent stage and identification of mRNA that is highly expressed during fungal quiescence. This application that includes the use of complementary strands (surface and reporter, Fig. 1) to these mRNAs, which are induced during quiescence, allows simple and sensitive visualization of gene induced

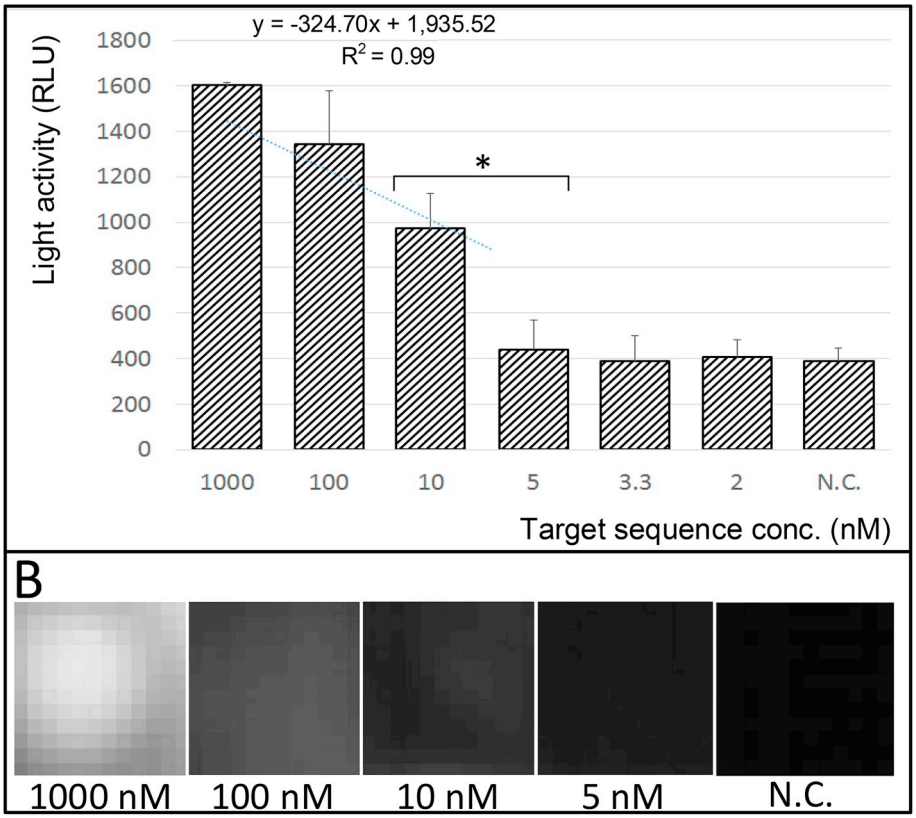

Fig. 5. (A) Response of the system to different concentrations of specific sequence Cgl_00014,454 (enoyl-CoA-hydratase/isomerase). *P < 0.005 by ANOVA. RLU, relative light units. (B) Visualization of the light activity on the surface of the tubes exposed to different concentrations of Cgl_00014,454. N.C., negative control.

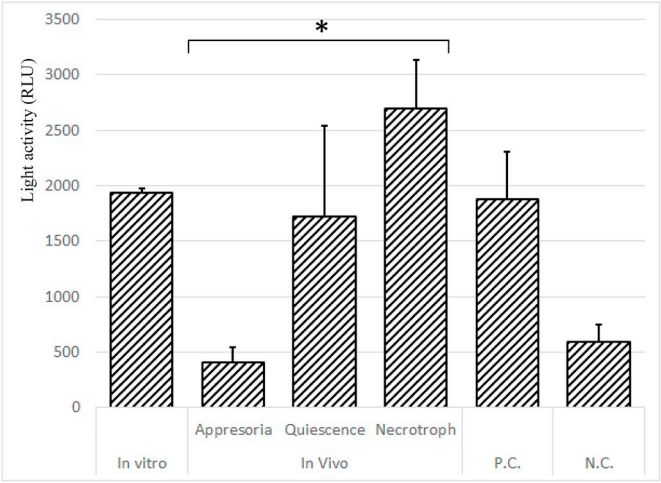

Fig. 6. Response of the system to total peel RNA at different *C. gloeosporioides*-infection stages. In parallel, the system was exposed to RNA extracted from fungus grown on the plate (*in vitro*) and to a synthetic DNA sample. RLU, relative light units; P·C., positive control; N·C., negative control. $*P < 0.005$ by ANOVA.

expression. Fig. 6 demonstrates the responses of the biosensor to the fungus *in vitro* (i.e., hyphal growth stage) and at three different *in-vivo* stages on tomato fruit—appressorium (penetration stage), quiescence (latent stage) and necrotrophic (pathogenic stage). In parallel, CMOS was exposed to the synthesized DNA sequence (as a positive control) and samples without target DNA (as a negative control). Quiescent and necrotrophic stages induced sensor responses compared to the appressorium stage (Fig. 6). The gene enoyl-CoA-hydratase/isomerase is highly induced during the quiescent stage, when the fungi are dormant and their metabolic and transcriptomic activities are significantly reduced [10]. Interestingly, the signal was also visible during necrotrophic and pathogenic colonization, when this specific gene is not induced but the fungi are highly active and proliferating (Fig. 6). The correlation between light intensity and DNA concentration in the sample was shown in section 3.3 (Fig. 5). Thus, during quiescence, mRNA transcription is induced, with more RNA hybridization to the immobilized surface and reporter DNA sequences and therefore a stronger light emission was observed. During active pathogenicity, the fungi will grow and proliferate, leading to similar light emission. These results show that the proposed system is not only able to determine the presence of the pathogens in fresh postharvest produce, but also senses fungi during their microscopic quiescent stage when their metabolism is reduced, while they are not visible to the naked eye.

4. Conclusions

This work presents a proof of concept of a novel CMOS-based biosensor for fungal detection in harvested crops. Moreover, the evaluation of the fungus inoculum rate, even during quiescent stage. Specificity and sensitivity of the technology were assessed with mRNA sequences isolated from *C. gloeosporioides*. In addition, the biosensor was able to distinguish between different pathogenicity stages. It is important to mention that, to the best of our knowledge, similar biosensors or other detection devices are not available for fungal pathogenicity in fresh produce, which are based on specific mRNA sequences corresponding to different stages of the fungal life cycle. There are numerous publications describing biosensors containing CMOS systems that are based on nucleic acids detection [47,48], but none directly address to identification of the stages (appressorium, quiescence or necrotrophic) of a disease or the life cycle of fungus. Furthermore, most of these reports describe pathogen-detecting devices for medical and clinical applications [16,49], and not for agricultural or food purposes. The unique ability of the proposed system to detect and recognize the fungus during both pathogenic and quiescent stages will decrease food losses by allowing improved postharvest management. For example, fruit with a high inoculum rate will be sold to the local market or as processed food, whereas fruit with low inoculum rates can be stored for long periods or exported.

Author contributions

Eltzov Evgeni (E.E.) and Noam Alkan (N.A.) developed the theory and performed proof of concept studies. E.E. and N.A. encouraged Dolev Zamir (D.Z.) to investigate the use of this concept for the determination capability of the system to detect and recognize the fungus during both pathogenic and quiescent stages. N.A. contributes his expertise in the field of the fungus-based postharvest diseases and E.E. in the biosensor field. Ortal Galsarker (O.G.) carried out all microbiology experiments and RNA extraction procedures. D.Z. carried out the biosensor experiments. All authors discussed the results and commented on the manuscript and contributed to the design and implementation of the research to the analysis of the results and the writing of the manuscript.

Funding

This research was supported by the Office of the Chief Scientist, Ministry of Agriculture and Rural Development (grant no. 16-10-0003).

Declaration of competing interest

The authors declared no potential conflicts of interest with respect to the research, authorship, and/or publication of this article.

Acknowledgments

The authors thank Dorin Harpaz for correcting the manuscript..

References

[1] K. Okawa, Market and Trade Impacts of Food Loss and Waste Reduction, (2015).
[2] Q. Zhou, D. Tang, Recent advances in photoelectrochemical biosensors for analysis of mycotoxins in food, Trac. Trends Anal. Chem. 124 (2020) 115814.
[3] Y. Fang, R.P. Ramasamy, Current and prospective methods for plant disease detection, Biosensors 5 (3) (2015) 537–561.
[4] S.N. Rahul, K. Khilari, S. Sagar, S. Chaudhary, S. Kumar, N. Vihan, A. Tomar, Challenges in postharvest management of fungal diseases in fruits and vegetables-a review, South Asian J. Food Technol. Environ 1 (2) (2015) 126–130.
[5] R. Dean, J.A.L. Van Kan, Z.A. Pretorius, K.E. Hammond-Kosack, A. Di Pietro, P.D. Spanu, J.J. Rudd, M. Dickman, R. Kahmann, J. Ellis, G.D. Foster, The Top 10 fungal pathogens in molecular plant pathology, Mol. Plant Pathol. 13 (4) (2012) 414–430.
[6] E. Fallik, Z. Ilić, Control of postharvest decay of fresh produce by heat treatments; the risks and the benefits, in: L. Palou, J.L. Smilanick (Eds.), Postharvest Pathology of Fresh Horticultural Produce, CRC press, Boca Raton, 2019, pp. 521–537.
[7] S. Droby, A. Lichter, Post-harvest Botrytis Infection: Etiology, Development and Management, Botrytis: Biology, Pathology and Control, Springer, 2007, pp. 349–367.
[8] L. Palou, Chapter 2 - Penicillium digitatum, Penicillium italicum (green mold, blue mold), in: S. Bautista-Baños (Ed.), Postharvest Decay, Academic Press, San Diego, 2014, pp. 45–102.
[9] D. Prusky, N. Alkan, T. Mengiste, R. Fluhr, Quiescent and necrotrophic lifestyle choice during postharvest disease development, Annu. Rev. Phytopathol. 51 (2013) 155–176.
[10] N. Alkan, G. Friedlander, D. Ment, D. Prusky, R. Fluhr, Simultaneous transcriptome analysis of Colletotrichum gloeosporioides and tomato fruit pathosystem reveals novel fungal pathogenicity and fruit defense strategies, New Phytol. 205 (2) (2015) 801–815.
[11] C.R.F. Caneira, R.R.G. Soares, I.F. Pinto, H.S. Mueller-Landau, A.M. Azevedo, V. Chu, J.P. Conde, Development of a rapid bead-based microfluidic platform for DNA hybridization using single- and multi-mode interactions for probe immobilization, Sensor. Actuator. B Chem. 286 (2019) 328–336.
[12] M. Mann, P. Hojrup, P. Roepstorff, Use of mass-spectrometric molecular-weight information to identify proteins in sequence databases, Biol. Mass Spectrom. 22 (6) (1993) 338–345.
[13] H. Shibata, J. Nemoto, S. Shiba, Y. Yamane, G. Kawai, K. Hashimoto,

Immobilization of DNA on quartz crystal microbalance sensor modified with self-assembled monolayer of thiol derivative, J. Oleo Sci. 69 (3) (2020) 271–276.
[14] K.A. Marx, Quartz crystal microbalance: a useful tool for studying thin polymer films and complex biomolecular systems at the solution− surface interface, Biomacromolecules 4 (5) (2003) 1099–1120.
[15] R.J. Baker, E. Institute of, E. Electronics, CMOS Circuit Design, Layout, and Simulation, (2005).
[16] N. Nikkhoo, N. Cumby, P.G. Gulak, K.L. Maxwell, Rapid bacterial detection via an all-electronic CMOS biosensor, PloS One 11 (9) (2016) e0162438.
[17] O. Tokel, U.H. Yildiz, F. Inci, N.G. Durmus, O.O. Ekiz, B. Turker, C. Cetin, S. Rao, K. Sridhar, N. Natarajan, H. Shafiee, A. Dana, U. Demirci, Portable microfluidic integrated plasmonic platform for pathogen detection, Sci. Rep. 5 (2015) 9152.
[18] T. Axelrod, E. Eltzov, R.S. Marks, Bioluminescent bioreporter pad biosensor for monitoring water toxicity, Talanta 149 (2016) 290–297.
[19] E. Eltzov, A. Cohen, R.S. Marks, Bioluminescent liquid light guide pad biosensor for indoor air toxicity monitoring, Anal. Chem. 87 (7) (2015) 3655–3661.
[20] Z. Ding, L. Liu, Y. Chung, Ultralow-Light CMOS Bio-Optical Sensor Enables Low-Cost, Portable Molecular Testing, LAURIN PUBL CO INC BERKSHIRE COMMON PO BOX 1146, PITTSFIELD, MA 01202 USA, 2017.
[21] S. Zhou, T. Gou, J. Hu, W. Wu, X. Ding, W. Fang, Z. Hu, Y. Mu, A highly integrated real-time digital PCR device for accurate DNA quantitative analysis, Biosens. Bioelectron. 128 (2019) 151–158.
[22] D. Tang, Y. Lin, Q. Zhou, Y. Lin, P. Li, R. Niessner, D. Knopp, Low-cost and highly sensitive immunosensing platform for aflatoxins using one-step competitive displacement reaction mode and portable glucometer-based detection, Anal. Chem. 86 (22) (2014) 11451–11458.
[23] Z. Gao, D. Tang, M. Xu, G. Chen, H. Yang, Nanoparticle-based pseudo hapten for target-responsive cargo release from a magnetic mesoporous silica nanocontainer, Chem. Commun. 50 (47) (2014) 6256–6258.
[24] W. Lai, Q. Wei, M. Xu, J. Zhuang, D. Tang, Enzyme-controlled dissolution of MnO2 nanoflakes with enzyme cascade amplification for colorimetric immunoassay, Biosens. Bioelectron. 89 (2017) 645–651.
[25] W. Lai, Q. Wei, J. Zhuang, M. Lu, D. Tang, Fenton reaction-based colorimetric immunoassay for sensitive detection of brevetoxin B, Biosens. Bioelectron. 80 (2016) 249–256.
[26] Y. Shang, J. Sun, Y. Ye, J. Zhang, Y. Zhang, X. Sun, Loop-mediated isothermal amplification-based microfluidic chip for pathogen detection, Crit. Rev. Food Sci. Nutr. 60 (2) (2020) 201–224.
[27] D. Chalupowicz, B. Veltman, S. Droby, E. Eltzov, Evaluating the use of biosensors for monitoring of Penicillium digitatum infection in citrus fruit, Sensor. Actuator. B Chem. 311 (2020) 127896.
[28] O. Kwon, T. Park, Applications of smartphone cameras in agriculture, environment, and food: a review, Journal of Biosystems Engineering 42 (4) (2017) 330–338.
[29] F. Algaar, E. Eltzov, M.M. Vdovenko, I.Y. Sakharov, L. Fajs, M. Weidmann, A. Mirazimi, R.S. Marks, Fiber-optic immunosensor for detection of crimean-Congo hemorrhagic fever IgG antibodies in patients, Anal. Chem. 87 (16) (2015) 8394–8398.
[30] E. Eltzov, D. Prilutsky, A. Kushmaro, R.S. Marks, C.D. Geddes, Metal-enhanced bioluminescence: an approach for monitoring biological luminescent processes, Appl. Phys. Lett. 94 (8) (2009).
[31] K. Aslan, Z. Leonenko, J.R. Lakowicz, C.D. Geddes, Fast and slow deposition of silver nanorods on planar Surfaces: application to metal-enhanced fluorescence, J. Phys. Chem. B 109 (8) (2005) 3157–3162.
[32] K. Aslan, I. Gryczynski, J. Malicka, E. Matveeva, J.R. Lakowicz, C.D. Geddes, Metal-enhanced fluorescence: an emerging tool in biotechnology, Curr. Opin. Biotechnol. 16 (1) (2005) 55–62.
[33] K. Aslan, Z. Leonenko, J.R. Lakowicz, C.D. Geddes, Annealed silver-island films for applications in metal-enhanced fluorescence: interpretation in terms of radiating plasmons, J. Fluoresc. 15 (5) (2005) 643.
[34] K. Wang, H. Peng, B. Wang, Recent advances in thiol and sulfide reactive probes, J. Cell. Biochem. 115 (6) (2014) 1007–1022.
[35] J.C. Lukesh, M.J. Palte, R.T. Raines, A potent, versatile disulfide-reducing agent from aspartic acid, J. Am. Chem. Soc. 134 (9) (2012) 4057–4059.
[36] A. Krężel, W. Leśniak, M. Jeżowska-Bojczuk, P. Młynarz, J. Brasuñ, H. Kozłowski, W. Bal, Coordination of heavy metals by dithiothreitol, a commonly used thiol group protectant, J. Inorg. Biochem. 84 (1) (2001) 77–88.
[37] G. Eidelshtein, N. Fardian-Melamed, V. Gutkin, D. Basmanov, D. Klinov, D. Rotem, Y. Levi-Kalisman, D. Porath, A. Kotlyar, Synthesis and properties of novel silver-containing DNA molecules, Adv. Mater. 28 (24) (2016) 4839–4844.
[38] Y. Fang, P.R. Ramasamy, Current and prospective methods for plant disease detection, Biosensors 5 (3) (2015).
[39] M. Ray, A. Ray, S. Dash, A. Mishra, K.G. Achary, S. Nayak, S. Singh, Fungal disease detection in plants: traditional assays, novel diagnostic techniques and biosensors, Biosens. Bioelectron. 87 (2017) 708–723.
[40] F. Cecchini, M. Manzano, Y. Mandabi, E. Perelman, R.S. Marks, Chemiluminescent DNA optical fibre sensor for Brettanomyces bruxellensis detection, J. Biotechnol. 157 (1) (2012) 25–30.
[41] R.K. Mendes, R.F. Carvalhal, D.R. Stach-Machado, L.T. Kubota, Surface plasmon resonance immunosensor for early diagnosis of Asian rust on soybean leaves, Biosens. Bioelectron. 24 (8) (2009) 2483–2487.
[42] R.K. Mendes, D.C.M. Ferreira, R.F. Carvalhal, L.A. Peroni, D.R. Stach-Machado, L.T. Kubota, Development of an electrochemical immunosensor for Phakopsora pachyrhizi detection in the early diagnosis of soybean rust, J. Braz. Chem. Soc. 20 (2009) 795–801.
[43] P. Wongkaew, S. Poosittisak, Diagnosis of sugarcane white leaf disease using the highly sensitive DNA based voltammetric electrochemical determination, Am. J. Plant Sci. 5 (15) (2014) 2256.
[44] A.J.-C. Eun, L. Huang, F.-T. Chew, S. Fong-Yau Li, S.-M. Wong, Detection of two orchid viruses using quartz crystal microbalance-based DNA biosensors, Phytopathology 92 (6) (2002) 654–658.
[45] G. Papadakis, N. Skandalis, A. Dimopoulou, P. Glynos, E. Gizeli, Bacteria murmur: application of an acoustic biosensor for plant pathogen detection, PloS One 10 (7) (2015) e0132773.
[46] E.R. Fossum, CMOS image sensors: electronic camera-on-a-chip, IEEE Trans. Electron. Dev. 44 (10) (1997) 1689–1698.
[47] S. MacKay, D. Wishart, J.Z. Xing, J. Chen, Developing trends in aptamer-based biosensor devices and their applications, IEEE Transactions on Biomedical Circuits and Systems 8 (1) (2014) 4–14.
[48] R. Thewes, F. Hofmann, A. Frey, B. Holzapfl, M. Schienle, C. Paulus, P. Schindler, G. Eckstein, C. Kassel, M. Stanzel, R. Hintsche, E. Nebling, J. Albers, J. Hassman, J. Schulein, W. Goemann, W. Gumbrecht, Sensor arrays for fully-electronic DNA detection on CMOS, 2002 IEEE International Solid-State Circuits Conference. Digest of Technical Papers (Cat. No.02CH37315), vol. 1, 2002, pp. 350–473.
[49] G.-J. Zhang, J.H. Chua, R.-E. Chee, A. Agarwal, S.M. Wong, Label-free direct detection of MiRNAs with silicon nanowire biosensors, Biosens. Bioelectron. 24 (8) (2009) 2504–2508.